Received May 2003
Revised June 2004
Accepted June 2004

The interaction of bioconvection caused by gyrotactic micro-organisms and settling of small solid particles

A.V. Kuznetsov and P. Geng
Department of Mechanical and Aerospace Engineering, North Carolina State University, Raleigh, North Carolina, USA

Abstract

Purpose – To investigate numerically the settling of small solid particles in a suspension of motile gyrotactic micro-organisms in order to evaluate the possibility of using bioconvection to slow down settling and enhance mixing between particles.

Design/methodology/approach – Numerical computations are performed at the North Carolina Supercomputing Center utilizing an Origin 2400 workstation. A conservative finite-difference scheme is used to discretize the governing equations. A staggered uniform grid with the stream function and vorticity stored in one set of nodes and the number densities of micro-organisms and solid particles stored in another set of nodes is utilized. CPU time required to investigate plume development until it attains steady-state for 36×36 uniform mesh is about 50 h.

Findings – It is established that small solid particles that are heavier than water slow down bioconvection. Extremely small particles (nanoparticles) that have negligible settling velocity do not have any noticeable impact on bioconvection, very large particles (that have negligible diffusivity), or very heavy particles (that have very large settling velocity) also do not have any impact on bioconvection because they simply settle at the bottom. However, if the particles are of the optimal size and density (gravitational settling must compete with Brownian diffusion to create an exponential number density distribution of solid particles with the maximum at the bottom of the chamber), these particles can effectively slow down bioconvection.

Research limitations/implications – The question how solid particles may affect the wavelengths of bioconvection patterns requires further investigation.

Practical implications – The finding that solid particles slow down bioconvection may be important in using bioconvection to enhance mixing in fluid microvolumes.

Originality/value – The paper provides a model and numerical data about the effect of bioconvection on mixing of small solid particles. These data are valuable for researches working in fundamental fluid mechanics, multiphase flow, and applications of bioconvection.

Keywords Particle size measurement, Sedimentary rocks, Motion, Micro-organisms

Paper type Research paper

International Journal of Numerical Methods for Heat & Fluid Flow
Vol. 15 No. 4, 2005
pp. 328-347

0961-5539
DOI 10.1108/09615530510590597

AVK gratefully acknowledges the grant # NAG3-2706 awarded to him by NASA Office of Biological and Physical Research, Physical Sciences Division. The authors also acknowledge the assistance of the North Carolina Supercomputing Center (NCSC) under an Advanced Computing Resources Grant. Critical comments of Professor D.A. Nield are greatly appreciated.

Nomenclature

a = radius of a micro-organism, m
B = time scale for the reorientation of micro-organisms by the gravitational torque against viscous torque, $4\pi\mu a^3/(mgh)$, s
D_m = diffusivity of micro-organisms, m^2/s
D_p = diffusivity of solid particles due to Brownian diffusion and interactions with micro-organisms, m^2/s
D_p^* = ratio of the diffusivity of solid particles to diffusivity of micro-organisms, D_p/D_m
$\mathbf{g}$ = gravity vector, 9.81 m/s^2
G = gyrotaxis number, BD_m/L^2
h = displacement of the center of mass of a gyrotactic micro-organism from its center of buoyancy, m
H = height of the chamber, m
J_m^* = dimensionless flux of micro-organisms, defined by equation (17a)
J_p^* = dimensionless flux of solid particles, defined by equation (17b)
L = width of the chamber, m
n_m = number density of micro-organisms, $1/m^3$
$\bar{n}_m$ = average number density of micro-organisms, $1/m^3$
n_m^* = dimensionless number density of micro-organisms, $n_m/\bar{n}_m$
n_p = number density of solid particles, $1/m^3$
$\bar{n}_p$ = average number density of solid particles, $1/m^3$
n_p^* = dimensionless number density of solid particles, $n_p/\bar{n}_m$
$\bar{n}_p^*$ = ratio of the average number density of particles to that of micro-organisms, $\bar{n}_p/\bar{n}_m$
$\hat{\mathbf{p}}$ = unit vector indicating the direction of swimming of gyrotactic micro-organisms
p_e = excess pressure (above hydrostatic), Pa
R_m = Rayleigh number for micro-organisms, $\bar{n}_m\theta_m\Delta\rho_m gL^3/(\rho_0\nu D_m)$
R_p = Rayleigh number for solid particles, $\bar{n}_m\theta_p\Delta\rho_p gL^3/(\rho_0\nu D_m)$
S_c = Schmidt number, ν/D_m
t = time, s
t^* = dimensionless time, $D_m t/L^2$
u = horizontal velocity component, m/s
v = vertical velocity component, m/s
$\mathbf{v}$ = velocity vector, m/s
W_m = average swimming velocity of micro-organisms (assumed to be constant), m/s
W_m^* = dimensionless average swimming velocity of micro-organisms, $W_m L/D_m$
W_p = particle settling velocity, m/s
W_p^* = dimensionless particle settling velocity, $W_p L/D_p$
x = horizontal coordinate, m
x^* = dimensionless horizontal coordinate, x/L
$\hat{\mathbf{x}}$ = unit vector in the x-direction
y = vertical coordinate, m
y^* = dimensionless vertical coordinate, y/L
$\hat{\mathbf{y}}$ = unit vector in the y-direction

Greek symbols

$\Delta\rho_m$ = density difference between micro-organisms and water, $\rho_m - \rho_0$, kg/m^3
$\Delta\rho_p$ = density difference between solid particles and water, $\rho_p - \rho_0$, kg/m^3
ζ = horizontal component of vorticity, 1/s
ζ^* = dimensionless horizontal component of vorticity, $\zeta L^2/D_m$
θ_m = volume of a micro-organism, m^3
θ_p = volume of a particle, m^3
Θ = angle between the vertical axis and the swimming velocity of micro-organisms
λ = aspect ratio of the chamber, H/L
μ = dynamic viscosity, assumed to be approximately the same as that of water, kg/(m s)
ν = kinematic viscosity, assumed to be approximately the same as that of water, m^2/s
ρ_0 = density of water, kg/m^3
ρ_m = density of micro-organisms, kg/m^3
ρ_p = density of solid particles, kg/m^3
ψ = stream function, m^2/s
ψ^* = dimensionless stream function, ψ/D_m

1. Introduction

Bioconvection is a phenomenon caused by collective swimming in a particular direction of motile micro-organisms. Most significant results in the area of bioconvection were obtained over the last two decades (Pedley *et al.*, 1988; Ghorai and Hill, 1999; Pedley and Kessler, 1987, 1990, 1992). Gyrotactic micro-organisms (this behavior is typical for many species of algae) swim against gravity in still water, but once bioconvection develops, their swimming direction is determined by the balance of two torques: the viscous torque acting on a body placed in a shear flow and the torque that is generated by gravity because the center of mass of a typical algae is displaced from its center of buoyancy. Algae are approximately 5 percent denser than water; gyrotactic behavior results in their swimming toward the regions of most rapid downflow. Therefore, the regions of downflow become denser than the regions of upflow. Buoyancy increases the upward velocity in the regions of upflow and downward velocity in the regions of downflow, thus enhancing velocity fluctuations and inducing macroscopic convective fluid motion (Pedley *et al.*, 1988; Ghorai and Hill, 1999, 2000). The formation of almost regular patterns and gyrotactic plumes in algal suspensions is documented in numerous experimental papers (Kessler, 1985a, b; Kessler *et al.*, 1997, 2000).

Despite a considerable number of theoretical and experimental works on bioconvection, the effect of bioconvection on settling of small solid particles has never been studied before. This is an interesting topic because it deals with a possible application of bioconvection: the utilization of bioconvection to slow down settling and enhance mixing between particles. The advantage of bioconvection is that it provides a simple mechanism for enhancing mixing and slowing down settling in very small fluid volumes (Ghorai and Hill, 1999, 2000, for example, studied bioconvection in a chamber as small as $5\,\text{mm} \times 5\,\text{mm}$). This may be important, for example, in the pharmaceutical industry or for the development of new medical tests. This statement implies micro-organisms not interfering with the test and surviving the presence of reactants.

This research is concentrated on investigating the settling of solid particles in a dilute suspension that contains both gyrotactic micro-organisms (whose number density is n_{m}) and small particles (whose density is n_{p}) in a two-dimensional chamber of depth H and width L whose side walls are assumed to be shear-free. Both micro-organisms and particles are heavier than water. The particles are small, so that the Brownian diffusion is not completely negligible. If diffusion were completely negligible, all particles would eventually end up at the bottom of the chamber. It is also assumed that particle diffusivity, caused by the Brownian motion, is enhanced by the interaction between the particles and the swimming micro-organisms. Because the suspension is dilute, this interaction is expected to be weak. Nevertheless, it cannot be completely neglected; therefore, it is modeled here by increasing the particle diffusivity as compared to its value predicted by the Einstein correlation. Stability analysis of this suspension is carried out in Kuznetsov and Avramenko (2004).

The computational domain is shown schematically in Figure 1(a). The width of the domain is L (the coordinate x varies from $-L/2$ to $L/2$) and the height of the domain is H (the coordinate y varies from 0 to H). The top boundary is assumed to be stress-free and the bottom boundary is rigid (the no-slip condition is imposed there). The side walls are stress-free to model periodic condition; a wider computational domain would

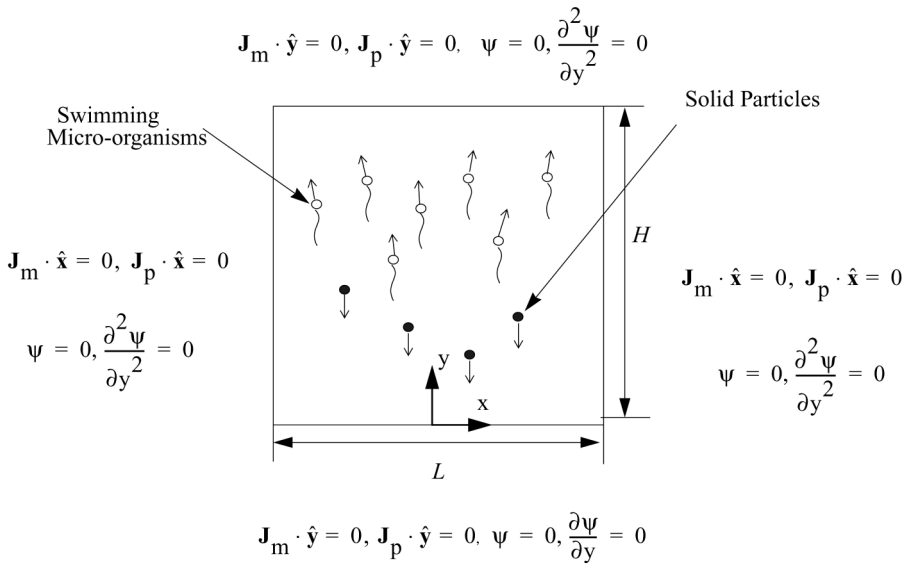

Figure 1.
(a) Computational domain and boundary conditions; and (b) swimming direction of a gyrotactic micro-organism

produce several identical plumes, it is assumed that the plume spacing is L. The question how solid particles may affect the wavelengths of bioconvection patterns requires further investigation.

2. Governing equations

2.1 Dimensional governing equations

Governing equations are written by extending equations given in Ghorai and Hill (1999, 2000) to account for solid particles. The cross-effect between micro-organisms

and solid particles movement is neglected because the suspension is dilute (volume concentrations of both micro-organisms and solid particles are much smaller than unity). Very slow motion associated with bioconvection flows justifies the creeping flow assumption and allows neglecting the inertia terms in these equations.

x- and y-momentum equations:

$$\rho_0 \frac{\partial u}{\partial t} = -\frac{\partial p_e}{\partial x} + \mu\left(\frac{\partial^2 u}{\partial x^2} + \frac{\partial^2 u}{\partial y^2}\right) \tag{1}$$

$$\rho_0 \frac{\partial v}{\partial t} = -\frac{\partial p_e}{\partial y} + \mu\left(\frac{\partial^2 v}{\partial x^2} + \frac{\partial^2 v}{\partial y^2}\right) - n_m \theta_m \Delta\rho_m g - n_p \theta_p \Delta\rho_p g \tag{2}$$

Continuity equation:

$$\frac{\partial u}{\partial x} + \frac{\partial v}{\partial y} = 0 \tag{3}$$

Conservation of motile micro-organisms:

$$\frac{\partial(n_m)}{\partial t} = -\mathrm{div}(n_m \mathbf{v} + n_m W_m \hat{\mathbf{p}} - D_m \nabla n_m) \tag{4}$$

Conservation of solid particles:

$$\frac{\partial(n_p)}{\partial t} = -\mathrm{div}\left(n_p \mathbf{v} + n_p W_p \frac{\mathbf{g}}{|\mathbf{g}|} - D_p \nabla n_p\right) \tag{5}$$

where D_m is the diffusivity of micro-organisms (this assumes that all random motions of the micro-organisms can be approximated by a diffusive process); D_p is the diffusivity of particles due to the Brownian motion and interactions with micro-organisms (D_p is smaller than D_m, but still not zero); n_m is the number density of motile micro-organisms; n_p is the number density of solid particles; p_e is the excess pressure above hydrostatic; $\hat{\mathbf{p}}$ is the unit vector indicating the direction of swimming of micro-organisms (equations for this vector are given in Pedley *et al.*, 1988); t is the time; u and v are the x- and y-velocity components, respectively; $\mathbf{v}$ is the velocity vector, (u,v); $W_m\hat{\mathbf{p}}$ is the vector of micro-organisms' average swimming velocity relative to the fluid (W_m is assumed to be constant); $W_p(\mathbf{g}/|\mathbf{g}|)$ is the vector of particles' settling velocity relative to the fluid (W_p is assumed to be constant, the particles settle straight downward); x and y are the Cartesian coordinates (x is the horizontal coordinate and y is the vertical coordinate); $\Delta\rho_m$ is the density difference between the micro-organisms and the water, $\rho_m - \rho_0$; $\Delta\rho_p$ is the density difference between the particles and the water, $\rho_p - \rho_0$; θ_m is the volume of a micro-organism; θ_p is the volume of a particle; μ is the dynamic viscosity, assumed to be approximately the same as that of water; and ρ_0 is the density of water.

For spherical particles the settling velocity can be found according to the Stokes law (Batchelor, 1982), as:

$$W_p = \frac{\theta_p \Delta\rho_p g}{6\pi\mu\left(\frac{3}{4}\frac{\theta_p}{\pi}\right)^{1/3}} \tag{6}$$

According to Ghorai and Hill (2000), vector $\hat{\mathbf{p}}$ that determines the swimming direction of a gyrotactic micro-organism can be given in terms of the angle Θ between the vertical axis and the vector of swimming velocity of the micro-organism (cf. Figure 1(b)), so that $\hat{\mathbf{p}} = (p_x, p_y) = (-\sin\Theta, \cos\Theta)$. Angle Θ satisfies the following equation:

$$\frac{\mathrm{d}\Theta}{\mathrm{d}t} = \frac{B\zeta - \sin\Theta}{2B} \tag{7}$$

where ζ is the horizontal component of vorticity and B is the time scale for the reorientation of micro-organisms by the gravitational torque against viscous resistance. Parameter B was called the "gyrotactic orientation parameter" by Pedley and Kessler (1987), it is defined as:

$$B = \frac{4\pi\mu a^3}{mgh} \tag{8}$$

where h is the displacement of the center of mass of a gyrotactic micro-organism from its center of buoyancy, m is the mass of the micro-organism, and a is the radius of the micro-organism.

2.2 Dimensionless governing equations

Utilizing the stream function-vorticity formulation, the governing equations can be recast in dimensionless form as follows:

$$\zeta^* = -\nabla^2\psi^* \tag{9}$$

$$S_c^{-1}\left(\frac{\partial\zeta^*}{\partial t^*} + u^*\frac{\partial\zeta^*}{\partial x^*} + v^*\frac{\partial\zeta^*}{\partial y^*}\right) = \nabla^2\zeta^* - \left(R_m\frac{\partial n_m^*}{\partial x^*} + R_p\frac{\partial n_p^*}{\partial x^*}\right) \tag{10}$$

$$\frac{\partial n_m^*}{\partial t^*} = -\nabla\cdot[n_m^*(\mathbf{v}^* + W_m^*\hat{\mathbf{p}}) - \nabla n_m^*] \tag{11}$$

$$\frac{\partial n_p^*}{\partial t^*} = -\nabla\cdot\left[n_p^*\left(\mathbf{v}^* + W_p^*\frac{\mathbf{g}}{|\mathbf{g}|}\right) - D_p^*\nabla n_p^*\right] \tag{12}$$

In Ghorai and Hill (1999, 2000) it is shown that vector $\hat{\mathbf{p}}$ can be computed as:

$$\hat{\mathbf{p}} = \begin{cases} (-\kappa - (\kappa^2 - 1)^{1/2}, 0), & \kappa < -1 \\ (-\kappa, (1 - \kappa^2)^{1/2}), & |\kappa| \le 1 \\ (-\kappa + (\kappa^2 - 1)^{1/2}, 0), & \kappa > 1 \end{cases} \tag{13}$$

where $\kappa = B\zeta = G\zeta^*$.

The dimensionless variables in equations (9)-(12) are:

$$x^* = \frac{x}{L};\quad y^* = \frac{y}{L};\quad t^* = \frac{D_m}{L^2}t;\quad u^* = \frac{\partial\psi^*}{\partial y^*};\quad v^* = -\frac{\partial\psi^*}{\partial x^*};\quad \mathbf{v}^* = \mathbf{v}\frac{L}{D_m};$$

$$W_{\mathrm{m}}^{*}=W_{\mathrm{m}}\frac{L}{D_{\mathrm{m}}};\quad W_{\mathrm{p}}^{*}=W_{\mathrm{p}}\frac{L}{D_{\mathrm{m}}};\quad n_{\mathrm{m}}^{*}=\frac{n_{\mathrm{m}}}{\bar{n}_{\mathrm{m}}};\quad n_{\mathrm{p}}^{*}=\frac{n_{\mathrm{p}}}{\bar{n}_{\mathrm{m}}};$$

$$S_{\mathrm{c}}=\frac{\nu}{D_{\mathrm{m}}};\quad G=\frac{BD_{\mathrm{m}}}{L^{2}};\quad R_{\mathrm{m}}=\frac{\bar{n}_{\mathrm{m}}\theta_{\mathrm{m}}\Delta\rho_{\mathrm{m}}gL^{3}}{\rho_{0}\nu D_{\mathrm{m}}};\quad R_{\mathrm{p}}=\frac{\bar{n}_{\mathrm{m}}\theta_{\mathrm{p}}\Delta\rho_{\mathrm{p}}gL^{3}}{\rho_{0}\nu D_{\mathrm{m}}};\tag{14}$$

$$D_{\mathrm{p}}^{*}=\frac{D_{\mathrm{p}}}{D_{\mathrm{m}}}$$

2.3 Initial and boundary conditions

Equations (9)-(12) must be solved subject to the following boundary conditions (cf. Figure 1(a)). No-slip boundary condition is imposed at the bottom wall while the top boundary and the side walls are assumed to be impermeable to the fluid and stress-free. The assumption that the top surface is stress-free implies that the surface tension is negligible and micro-organisms do not form a packed layer at the top surface. Under these assumptions the boundary conditions can be presented as:

$$\psi^{*}=0\ \text{at}\ y^{*}=0,\lambda\ \text{and}\ x^{*}=\pm 0.5,\tag{15a}$$

where λ is the aspect ratio, H/L,

$$\frac{\partial\psi^{*}}{\partial y^{*}}=0\ \text{at}\ y^{*}=0,\tag{15b}$$

$$\frac{\partial^{2}\psi^{*}}{\partial y^{*2}}=0\ \text{at}\ y^{*}=\lambda,\ \text{and}\ \frac{\partial^{2}\psi^{*}}{\partial x^{*2}}=0\ \text{at}\ x^{*}=\pm 0.5.\tag{15c}$$

All four boundaries of the domain are also impermeable to the fluid, micro-organisms, and solid particles; therefore, normal fluxes of micro-organisms and solid particles are zero through all these boundaries:

$$\mathbf{J}_{\mathrm{m}}^{*}\cdot\hat{\mathbf{y}}=0\ \text{and}\ \mathbf{J}_{\mathrm{p}}^{*}\cdot\hat{\mathbf{y}}=0\ \text{at}\ y^{*}=0,\lambda\tag{16a}$$

$$\mathbf{J}_{\mathrm{m}}^{*}\cdot\hat{\mathbf{x}}=0\ \text{and}\ \mathbf{J}_{\mathrm{p}}^{*}\cdot\hat{\mathbf{x}}=0\ \text{at}\ x^{*}=\pm 0.5,\tag{16b}$$

where $\hat{\mathbf{x}}$ and $\hat{\mathbf{y}}$ are the unit vectors in the x- and y-directions, respectively,

$$\mathbf{J}_{\mathrm{m}}^{*}=n_{\mathrm{m}}^{*}(\mathbf{v}^{*}+W_{\mathrm{m}}^{*}\hat{\mathbf{p}})-\nabla n_{\mathrm{m}}^{*}\tag{17a}$$

is the dimensionless flux of micro-organisms and

$$\mathbf{J}_{\mathrm{p}}^{*}=n_{\mathrm{p}}^{*}\left(\mathbf{v}^{*}+W_{\mathrm{p}}^{*}\frac{\mathbf{g}}{|\mathbf{g}|}\right)-D_{\mathrm{p}}^{*}\nabla n_{\mathrm{p}}^{*}\tag{17b}$$

is the dimensionless flux of solid particles.

Initially, at $t^{*}=0$, it is assumed that the fluid is motionless and the number density distributions of micro-organisms and solid particles are uniform. As in Ghorai and Hill (1999, 2000), small perturbations to these uniform distributions are utilized to ensure

that the plume forms in the middle of the computational domain. This results in the following initial condition:

$$\psi^* = 0, \quad \zeta^* = 0, \quad n_{\mathrm{m}}^* = 1 + \varepsilon \cos(m\pi x^*), \quad n_{\mathrm{p}}^* = \frac{\bar{n}_{\mathrm{p}}}{\bar{n}_{\mathrm{m}}} + \varepsilon \cos(m\pi x^*) \tag{18}$$

where $\varepsilon = 10^{-5}$ and $m = 2$.

2.4 Numerical procedure

A conservative finite-difference scheme is used to discretize the governing equations. An implicit scheme with Euler backward differencing in time and central differencing in space is utilized to obtain the transient solutions. A line-by-line tridiagonal matrix algorithm with relaxation is used together with an iteration technique to solve the nonlinear discretized equations. A staggered uniform grid with the stream function and vorticity stored in one set of nodes and the number densities of micro-organisms and solid particles stored in another set of nodes is utilized. The grid is chosen so that the number density nodes lie in the interior of the computational domain only, whereas those of the stream function and vorticity lie in the interior and at the boundary of the domain. The mesh size is 36×36. Computations are performed at the North Carolina Supercomputing Center utilizing an Origin 2400 workstation. CPU time required to investigate plume development until it attains steady-state for 36×36 uniform mesh is about 50 h. Grid independence of the solution was checked by performing a test computation utilizing a uniform 72×72 mesh, and the maximum variation of the fluid velocity did not exceed 3 percent.

3. Results and discussion

Values of physical properties and geometrical parameters utilized in the computations are summarized in Table I. Values of dimensionless groups that correspond to these parameter values are given in Table II. The values of particle diffusivity are taken larger than those following from the Einstein's relation that determines the diffusivity of small particles due to the Brownian motion. This is done to account for additional random motions of particles that may result from their interactions with swimming micro-organisms (a particle may be either directly hit by a micro-organism or it can enter a propulsive stream caused by a swimming micro-organism).

The major aim of the presented computations is to investigate the effect of solid particles on bioconvection as well as the effect of bioconvection on number density distribution of solid particles in the chamber. Without bioconvection, solid particles have exponential distribution across the chamber's depth with the largest number density at the bottom of the chamber (the particles do not all settle to the bottom because of the Brownian diffusion). The particle number density distribution can be obtained by integrating equation (12) for the case when $\mathbf{v}^* = \partial n_{\mathrm{p}}^*/\partial t^* = 0$, as:

$$n_{\mathrm{p}}^*(y^*) = -\frac{1}{D_{\mathrm{p}}^*} \frac{\exp\left(-\frac{1}{D_{\mathrm{p}}^*} W_{\mathrm{p}}^* y^*\right) - 1}{\exp\left(-\frac{1}{D_{\mathrm{p}}^*} W_{\mathrm{p}}^*\right) - 1} \bar{n}_{\mathrm{p}}^* W_{\mathrm{p}}^* \tag{19}$$

To evaluate the effect of solid particles on bioconvection, the basic case when there are no solid particles in the suspension is first investigated. Figure 2(a)-(d) shows the

Average number density of micro-organisms	$\bar{n}_m$	10^{12} cells/m^3
Average number density of solid particles	$\bar{n}_p$	10^{11} cells/m^3
Density of water	ρ_0	10^3 kg/m^3
Specific gravity of micro-organisms	$\Delta\rho_m/\rho_0$	0.05
Specific gravity of solid particles	$\Delta\rho_p/\rho_0$	Figures 3-8: 0. 25 Figure 9: 0.5 Figure 10: 1
Volume of a micro-organism	θ_m	5×10^{-16} m^3
Volume of a particle	θ_p	5×10^{-16} m^3
Average swimming velocity of micro-organisms	W_c	10^{-4} m/s
Particle settling velocity (calculated according to equation (6))	W_p	Figures 3-8: 1.32×10^{-5} m/s Figure 9: 2.64×10^{-5} m/s Figure 10: 5.28×10^{-5} m/s
Diffusivity of micro-organisms	D_m	5×10^{-8} m^2/s
Diffusivity of particles	D_p	Figures 3-6, 9, 10: 5×10^{-9} m^2/s Figure 7: 1×10^{-8} m^2/s Figure 8: 5×10^{-8} m^2/s
Gyrotaxis orientation parameter	B	5 s
Kinematic viscosity of the suspension	ν	10^{-6} m^2/s
Height of the computational domain	H	0.005 m
Width of the computational domain	L	0.005 m

Table I.
Physical properties and geometrical parameters utilized in the computations

Dimensionless average swimming velocity of micro-organisms	$W^*_m = W_m(L/D_m)$	10^{-2}
Dimensionless particles settling velocity	$W^*_p = W_p(L/D_m)$	Figures 3-8: 1.32×10^{-3} Figure 9: 2.64×10^{-3} Figure 10: 5.28×10^{-3}
Schmidt number	$S_c = \nu/D_m$	20
Gyrotaxis number	$G = BD_m/L^2$	10^{-2}
Rayleigh number for micro-organisms	$R_m = \bar{n}_m\theta_m\Delta\rho_m gL^3/\rho_0\nu D_m$	612.5
Rayleigh number for solid particles	$R_p = \bar{n}_m\theta_p\Delta\rho_p gL^3/\rho_0\nu D_m$	Figures 3-8: 3062.5 Figure 9: 6125 Figure 10: 12250
Dimensionless diffusivity of particles	$D^*_p = D_p/D_m$	Figures 3-6, 9, 10: 0.1 Figure 7: 0.2 Figure 8: 1
Aspect ratio	$\lambda = H/L$	1
Dimensionless average concentration of particles	$\bar{n}^*_p = \bar{n}_p/\bar{n}_m$	0.1

Table II.
Values of dimensionless parameters utilized in computations

dimensionless number density of micro-organisms (a), the contours of the dimensionless stream function (b), the fluid velocity vector filed (c), and the flow streamlines (d) for the case of no solid particles when bioconvection plume attains its steady-state (as shown below, this happens at $t^* = 0.49825$).

Figures 3-6 display the case with solid particles, computations are carried out for $\Delta\rho_p/\Delta\rho_m = 5$ and $D_p/D_m = 0.1$. As shown in Table II, for all computations with particles it is assumed that the average number density of particles is ten times smaller than that of micro-organisms, $\bar{n}_p/\bar{n}_m = 0.1$. Since the case with solid particles is of major interest for this investigation, Figures 3-6 show the development of the

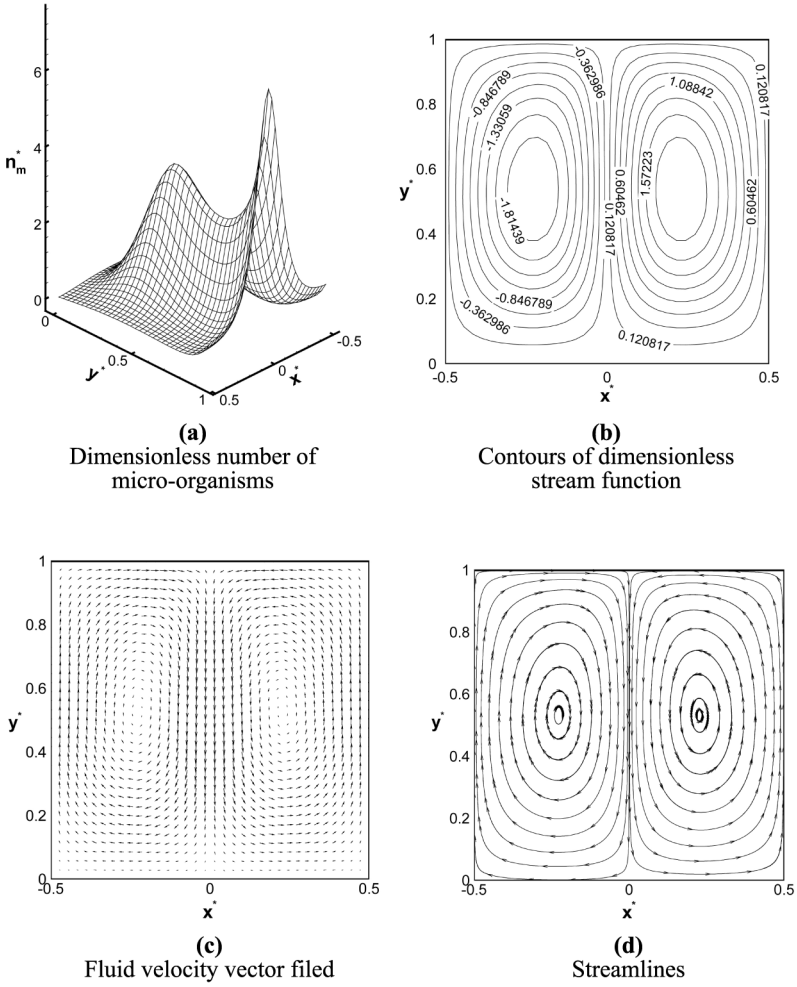

Figure 2.
Basic case: no solid particles, steady-state plume ($t^* = 0.49825$)

bioconvection plume: Figure 3 shows the plume at $t^* = 0.19825$, Figure 4 shows the plume at $t^* = 0.3$, Figure 5 at $t^* = 0.49825$, and Figure 6 at $t^* = 0.59825$. In Figures 3-6, Figure (a) shows the dimensionless number density of micro-organisms, Figure (b) shows the dimensionless number density of particles, Figure (c) shows contours of the dimensionless stream function, and Figure (d) shows the fluid velocity vector field. Table III shows the maximum values of the dimensionless number densities of micro-organisms and particles, $(n^*_{\mathrm{m}})_{\max}$ and $(n^*_{\mathrm{p}})_{\max}$, and the maximum value of the dimensionless stream function, $(\psi^*)_{\max}$. As Table III shows, these three parameters change by no more than 2.3 percent between $t^* = 0.49825$ and 0.59825. Therefore, it is assumed that at $t^* = 0.49825$, the plume attains its steady state.

Figures 7 and 8 display the steady-state bioconvection plumes for the case of $\Delta\rho_{\mathrm{p}}/\Delta\rho_{\mathrm{m}} = 5$ when $D_{\mathrm{p}}/D_{\mathrm{m}} = 0.2$ and 1, respectively. Table IV summarizes the maximum values of the dimensionless number densities of micro-organisms and

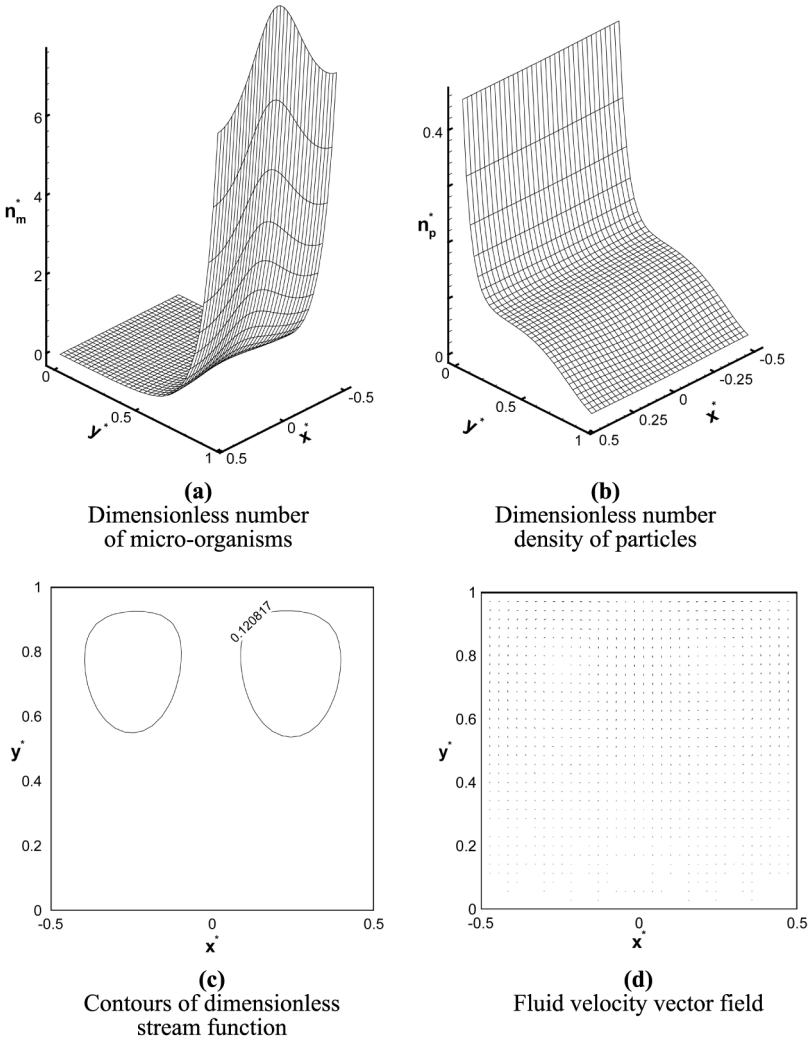

Figure 3.
Solid particles present, $\bar{n}_p/\bar{n}_m = 0.1$, $\Delta\rho_p/\Delta\rho_m = 5$, $D^*_p/D_m = 0.1$, $t^* = 0.19825$

particles, $(n^*_m)_{max}$ and $(n^*_p)_{max}$, and the maximum value of the dimensionless stream function, $(\psi^*)_{max}$, for the basic case of no solid particles (Figure 2) and cases with solid particles (Figures 5, 7, and 8) for different diffusivities of the particles (all cases with particles shown in Table IV are computed for $\Delta\rho_p/\Delta\rho_m = 5$). Number density of micro-organisms takes on its maximum value at the top of the computational domain, while number density of solid particles takes on its maximum value at the bottom of the domain. According to boundary conditions (equation (15a)), the stream function takes on zero value at the boundaries of the domain. Since the stream function field is similar for all computed cases, the maximum value of the stream function indicates, on average, how strong the fluid velocity in the domain is. Figures 5, 7, and 8 and Table IV show that the increase of diffusivity of solid particles results in a more uniform

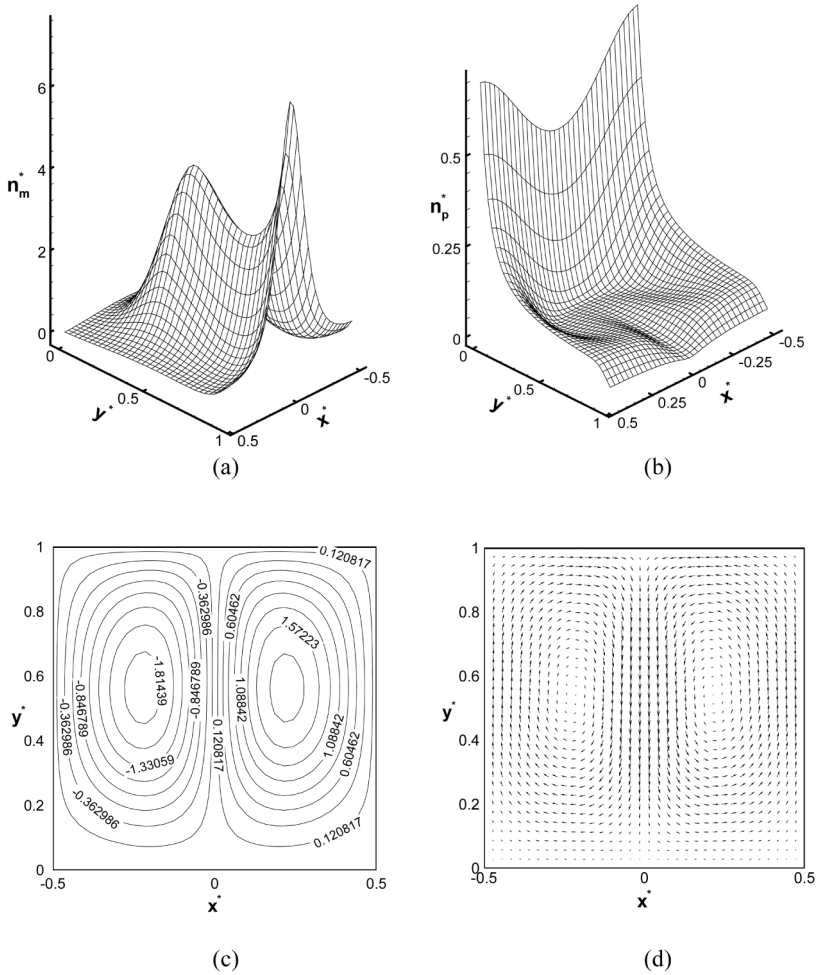

Figure 4.
Solid particles present, $\bar{n}_p/\bar{n}_m = 0.1$, $\Delta\rho_p/\Delta\rho_m = 5$, $D_p/D_m = 0.1$, $t^* = 0.3$. (a) Dimensionless number density of micro-organisms, (b) dimensionless number density of particles, (c) contours of the dimensionless stream function, (d) fluid velocity vector field

distribution of the particles over the depth of the chamber. A much more interesting conclusion is obtained by comparing the values of $(\psi^*)_{max}$ for the case of no solid particles and the cases with solid particles of different diffusivities. For all computed cases, the value of $(\psi^*)_{max}$ is the largest for the case with no solid particles, which indicates that the presence of solid particles slows down bioconvection. Bioconvection is slowed down more efficiently by larger particles that, according to the Einstein relation, have smaller diffusivity and, therefore, concentrate near the bottom of the chamber. This unexpected result has a simple physical explanation. Bioconvection is caused by unstable density stratification that is created by the upswimming of micro-organisms that are heavier than water. Very small particles (nanoparticles) that have very large diffusivity and whose distribution across the depth of the chamber is almost uniform have no impact on density stratification and, therefore, have no impact on bioconvection. Larger particles with smaller diffusivity concentrate near the bottom

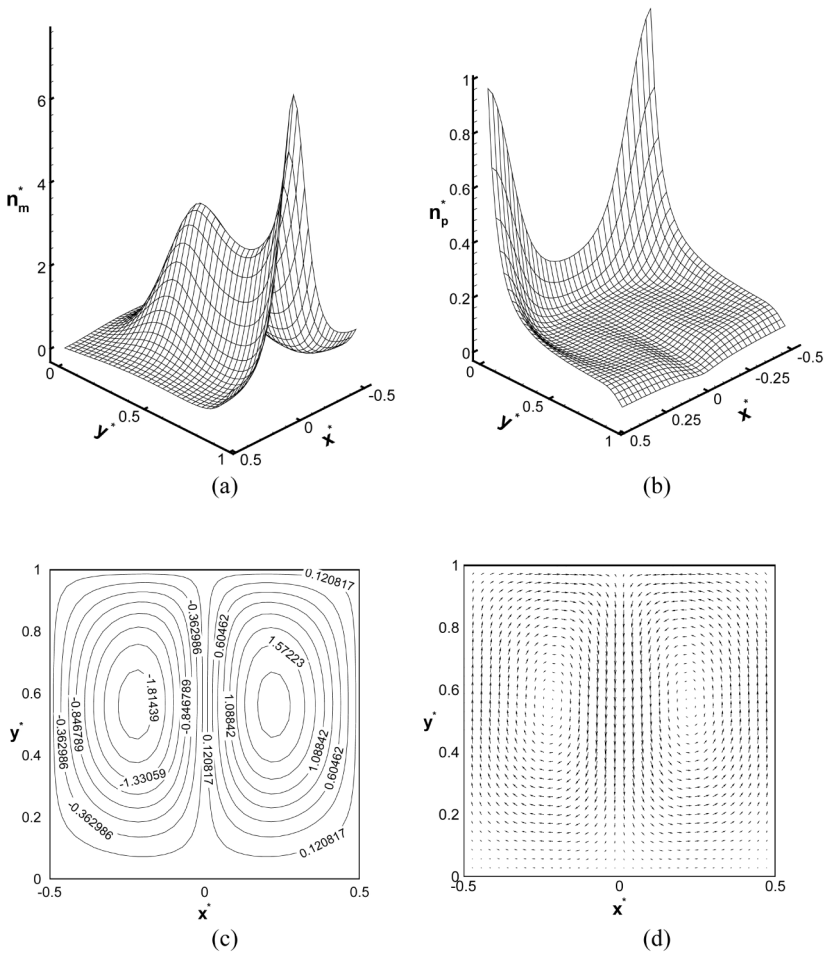

Figure 5.
Solid particles present, $\bar{n}_p/\bar{n}_m = 0.1$, $\Delta\rho_p/\Delta\rho_m = 5$, $D^*_p/D_m = 0.1$, $t^* = 0.49825$: (a) dimensionless number density of micro-organisms; (b) dimensionless number density of particles; (c) contours of the dimensionless stream function; and (d) fluid velocity vector field

of the chamber. Since the particles are heavier than water, they create a more stable density stratification partly compensating for the increase of density in the upper fluid layer caused by the upswimming of micro-organisms. Therefore, larger particles slow down bioconvection more effectively than very small particles. Figure 9(a) shows number density distributions of small particles at steady-state computed for two cases: with no bioconvection (computed utilizing equation (19)) and with bioconvection (in this case number density distribution is shown in the middle of the chamber, at $x^* = 0$). Number density distributions shown in Figure 9(a) correspond to the cases that are displayed in Figures 5, 7, and 8 and summarized in Table IV. In can be seen that if particle diffusivity is very large (the case of $D_p/D_m = 1$), the number density distribution of such solid particles across the depth of the chamber is almost uniform, which explains why these particles do not have considerable impact on bioconvection. However, the conclusion that larger particles slow down bioconvection is true only if the particles are not very large (which would imply that they have negligible

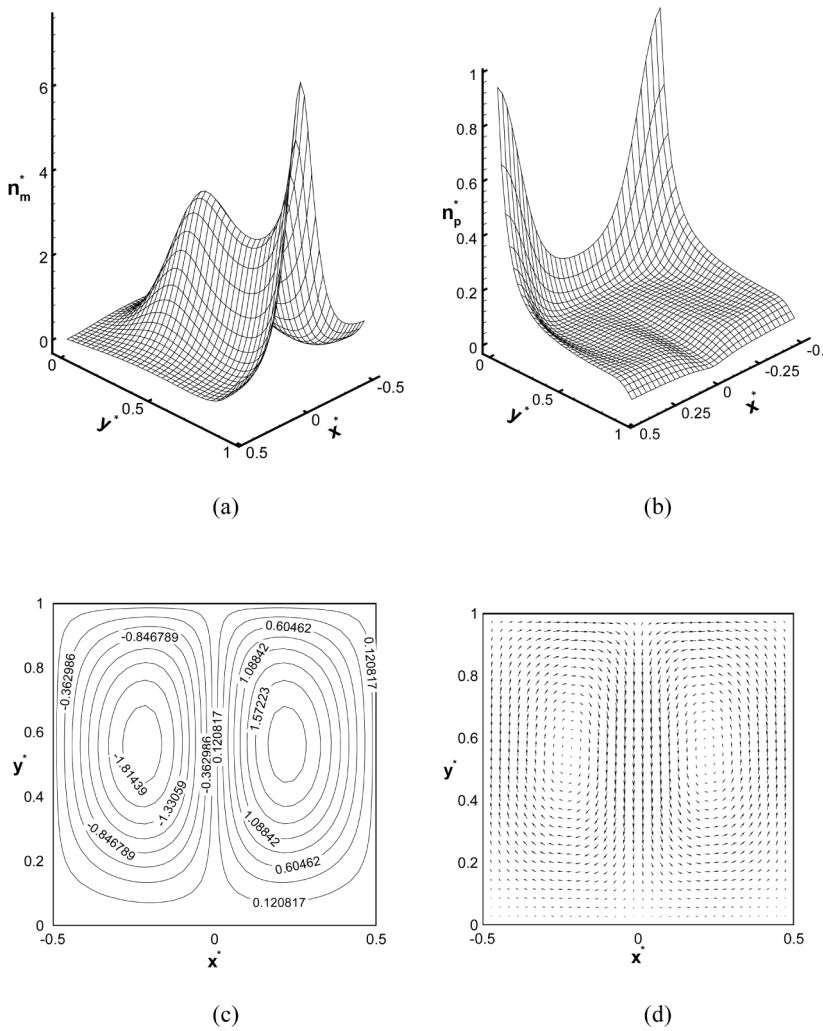

Figure 6.
Solid particles present, $\bar{n}_p/\bar{n}_m = 0.1$, $\Delta\rho_p/\Delta\rho_m = 5$, $D^*_p/D_m = 0.1$, $t^* = 0.59825$: (a) dimensionless number density of micro-organisms; (b) dimensionless number density of particles; (c) contours of the dimensionless stream function; and (d) fluid velocity vector field

t^*	$(n^*_m)_{max}$	$(n^*_p)_{max}$	$(\psi^*)_{max}$
0.19825	10.0561	0.453481	0.213259
0.30000	6.90995	0.700287	2.05947
0.49825	7.38435	0.962994	1.9235
0.59825	7.37157	0.941157	1.95196

Notes: Maximum values of the dimensionless number densities of micro-organisms and particles, as well as the maximum value of the dimensionless stream function in the computational domain for the case of $\Delta\rho_p/\Delta\rho_m = 5$ and $D^*_p = 0.1$ at different time (based on the data shown in Figures 3-6)

Table III.

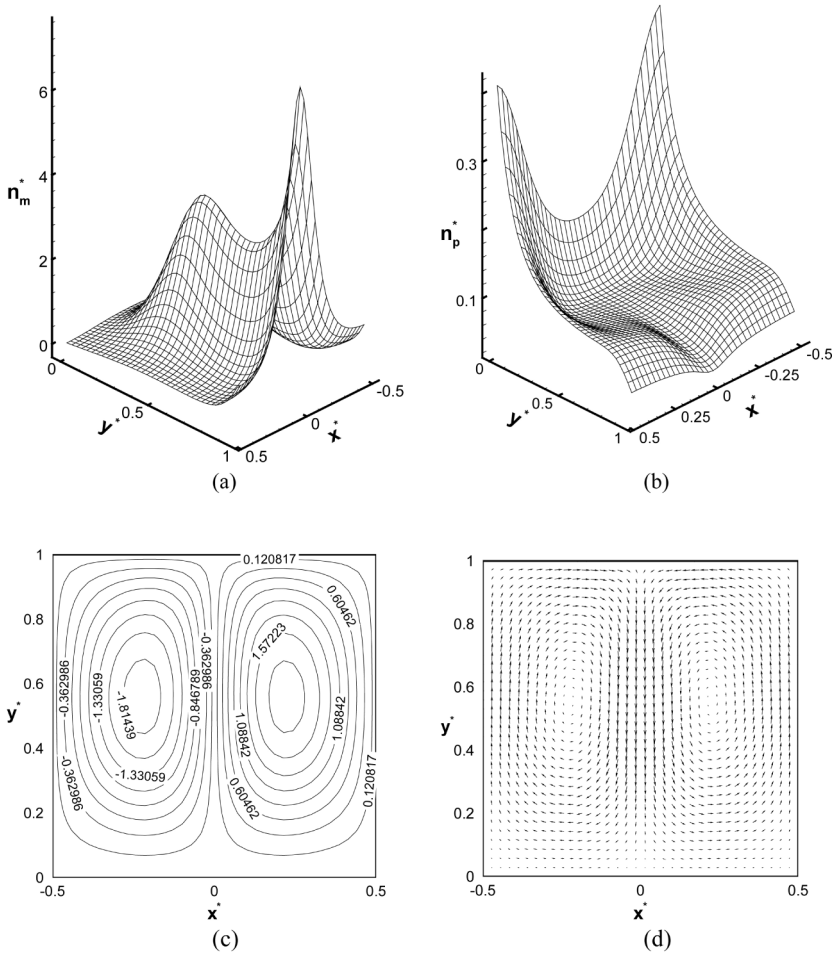

Figure 7.
Solid particles present, $\bar{n}_p/\bar{n}_m = 0.1$, $\Delta\rho_p/\Delta\rho_m = 5$, $D_p/D_m = 0.2$ and $t^* = 0.49825$ (steady-state plume): (a) dimensionless number density of micro-organisms; (b) dimensionless number density of particles; (c) contours of the dimensionless stream function; and (d) fluid velocity vector field

diffusivity) or very heavy (which would imply that they have very large settling velocity). Such particles do not have any impact on bioconvection because they simply settle down to the bottom. This means that there is an optimum size (optimum diffusivity) of solid particles when they slow down bioconvection most efficiently.

Figures 10 and 11 display the steady-state bioconvection plumes for the case of $D_p/D_m = 0.1$ when $\Delta\rho_p/\Delta\rho_m = 10$ and 20, respectively. Table V summarizes the maximum values of the dimensionless number densities of micro-organisms and particles, $(n^*_m)_{max}$ and $(n^*_p)_{max}$, and the maximum value of the dimensionless stream function, $(\psi^*)_{max}$, for the basic case of no solid particles (Figure 2) and cases with solid particles (Figures 5, 10, and 11) for different densities of the particles (all cases with particles shown in Table V are computed for $D_p/D_m = 0.1$). Table V shows that when particles become too heavy and, therefore, settle too fast, they have almost no impact on bioconvection. Number density distributions of solid particles in the middle of the

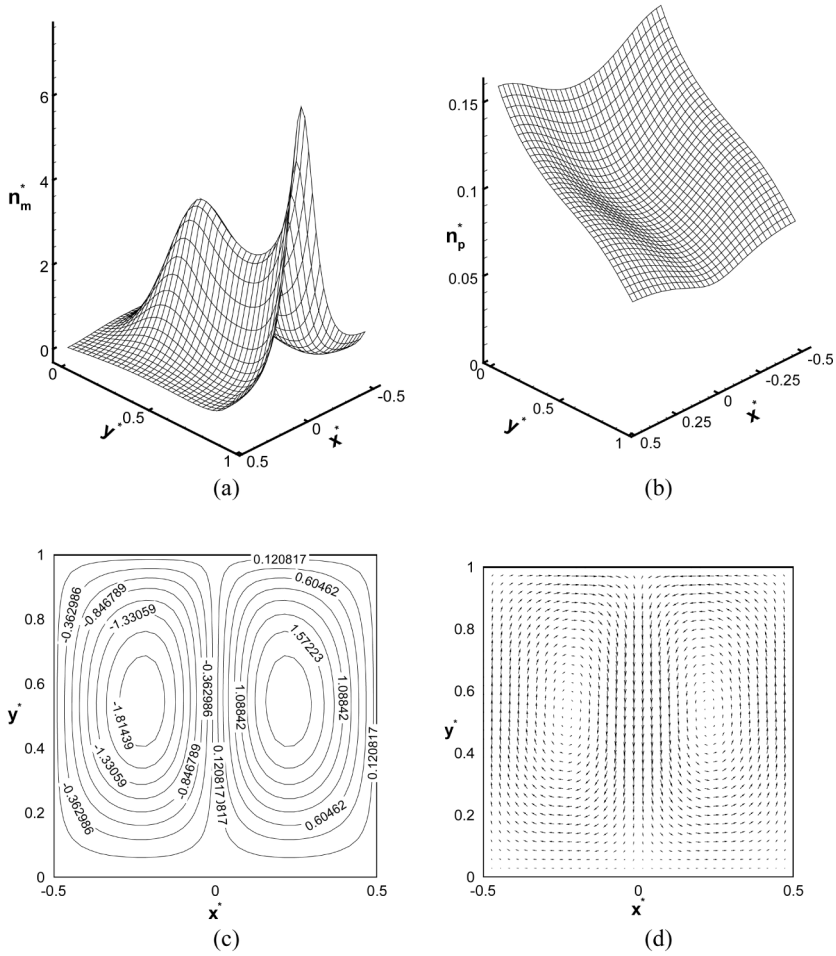

Figure 8.
Solid particles present, $\bar{n}_p/\bar{n}_m = 0.1$, $\Delta\rho_p/\Delta\rho_m = 5$, $D_p/D_m = 1$ and $t^* = 0.49825$ (steady-state plume): (a) dimensionless number density of micro-organisms; (b) dimensionless number density of particles; (c) contours of the dimensionless stream function; and (d) fluid velocity vector field

	$(n^*_m)_{max}$	$(n^*_p)_{max}$	$(\psi^*)_{max}$
No solid particles	6.79392	0	2.05603
$D_p/D_m=1$	7.01507	0.158789	2.00139
$D_p/D_m=0.2$	7.36259	0.410833	1.93294
$D_p/D_m=0.1$	7.38435	0.962994	1.9235

Notes: Maximum values of the dimensionless number densities of micro-organisms and particles, as well as the maximum value of the dimensionless stream function in the computational domain at steady-state conditions for $\Delta\rho_p/\Delta\rho_m = 5$ for different diffusivities of solid particles (based on the data shown in Figures 2, 5, 7, and 8)

Table IV.

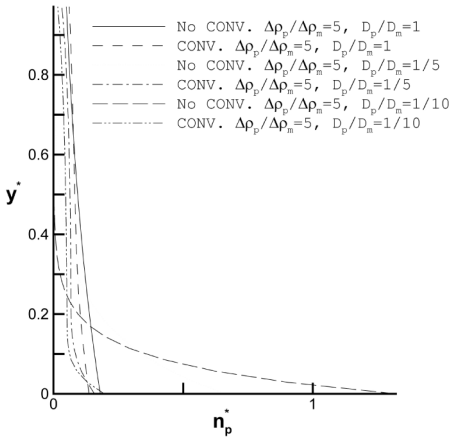

(a)

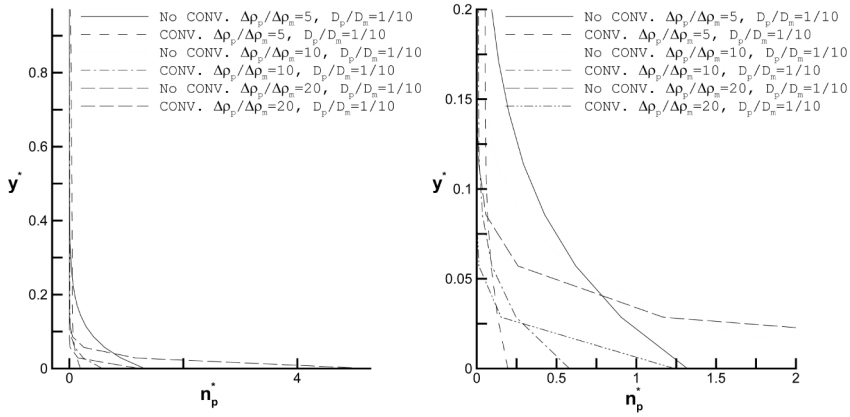

(b1) (b2)

Figure 9.
Distributions of the dimensionless number density of solid particles in the middle of the chamber (at $x^* = 0$) computed with no bioconvection and with bioconvection

Notes: (a) n_p^* at $x^* = 0$ for cases displayed in Figs. 5, 7, and 8; (b1) n_p^* at $x^* = 0$ for cases displayed in Figs. 5, 10, and 11; (b2) Same as (b1), enlarged scale to show number density of solid particles close to the bottom of the chamber

chamber that are shown in Figures 9(b1, b2) correspond to the cases that are displayed in Figures 5, 10, and 11 and summarized in Table V. (Figure 9(b2) shows number density distributions of solid particles close to the bottom of the chamber on an enlarged scale.) Figure 9(b1, b2) shows that heavy particles, because of their large settling velocity, just concentrate near the bottom of the chamber (there are almost no particles in the rest of the domain). This explains why very heavy particles (the case of $\Delta\rho_p/\Delta\rho_m = 20$) have almost no impact on bioconvection.

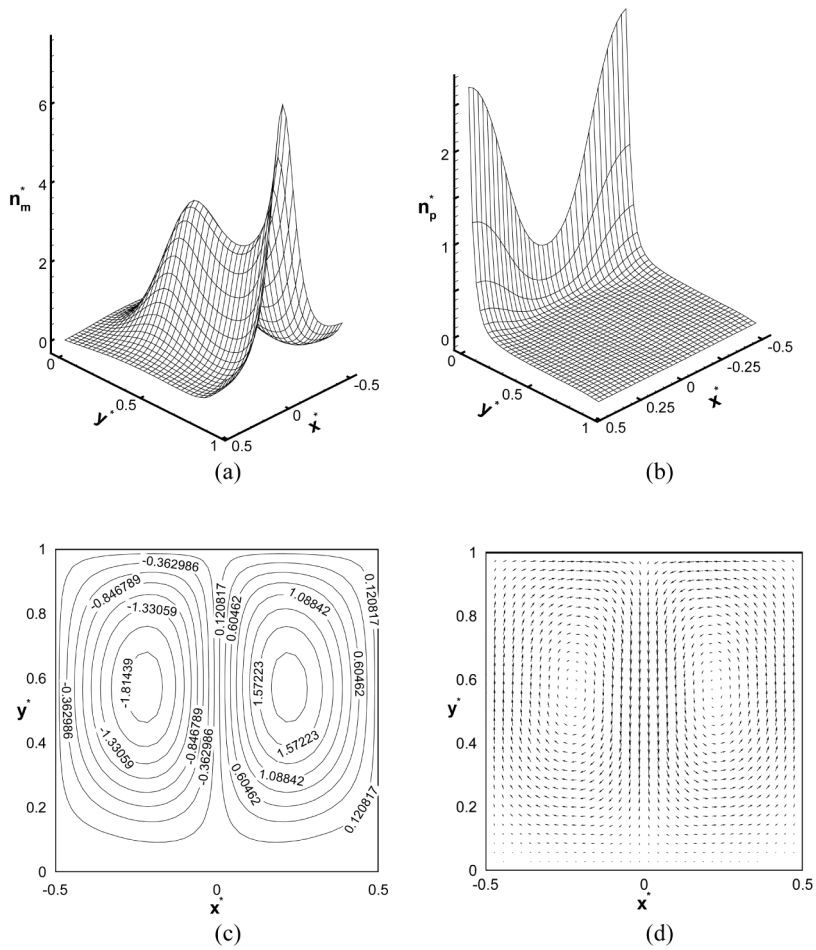

Figure 10.
Solid particles present, $\bar{n}_p/\bar{n}_m = 0.1$, $\Delta\rho_p/\Delta\rho_m = 10$, $D_p/D_m = 0.1$, and $t^* = 0.49825$ (steady-state plume): (a) dimensionless number density of micro-organisms; (b) dimensionless number density of particles; (c) contours of the dimensionless stream function; and (d) fluid velocity vector field

4. Conclusions

It is established that small solid particles that are heavier than water slow down bioconvection. This is attributed to the fact that solid particles create a more stable density stratification than micro-organisms alone. Extremely small particles (nanoparticles) that have negligible settling velocity do not have any noticeable impact on bioconvection, very large particles (that have negligible diffusivity) or very heavy particles (that have very large settling velocity) also do not have any impact on bioconvection because they simply settle at the bottom. However, if the particles are of the optimal size and density (gravitational settling must compete with Brownian diffusion to create an exponential number density distribution of solid particles with the maximum at the bottom of the chamber), these particles can effectively slow down bioconvection. On the other hand, bioconvection makes number density distribution of solid particles more uniform. Further experimental research is needed to confirm the theoretical predictions of this paper.

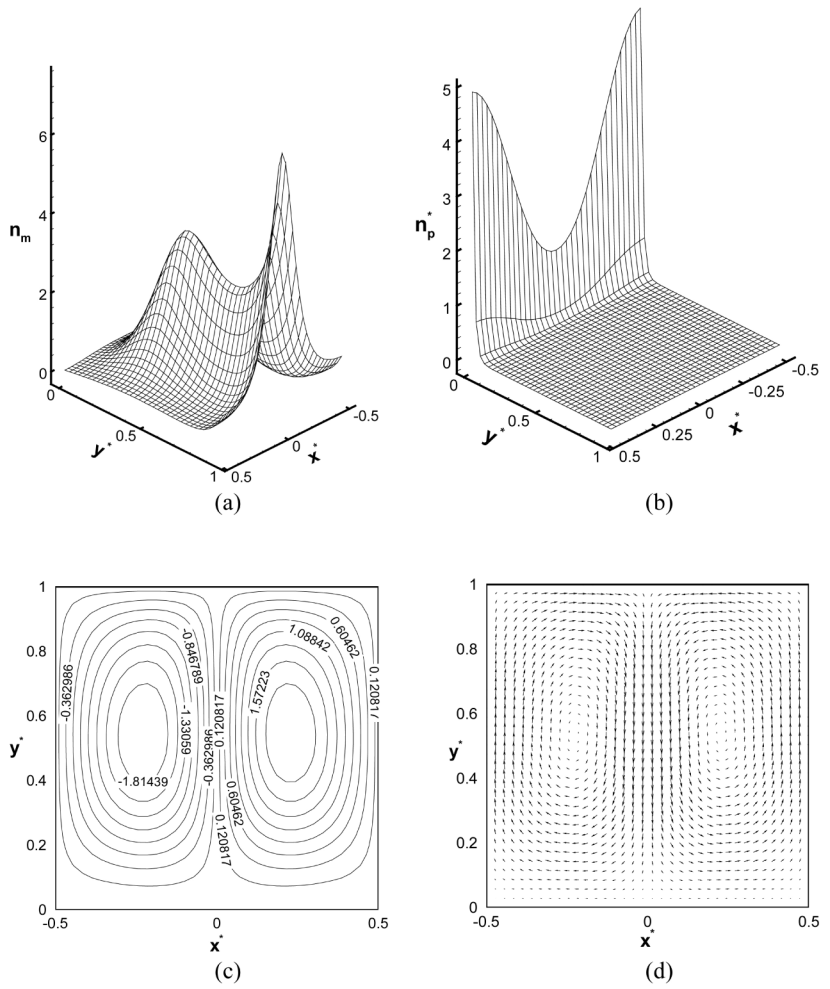

Figure 11.
Solid particles present, $\bar{n}_p/\bar{n}_m = 0.1$, $\Delta\rho_p/\Delta\rho_m = 20$, $D_p/D_m = 0.1$, and $t^* = 0.49825$ (steady-state plume): (a) dimensionless number density of micro-organisms; (b) dimensionless number density of particles; (c) contours of the dimensionless stream function; and (d) fluid velocity vector field

	$(n^*_m)_{max}$	$(n^*_p)_{max}$	$(\psi^*)_{max}$
No solid particles	6.79392	0	2.05603
$\Delta\rho_p/\Delta\rho_m$=5	7.38435	0.962994	1.9235
$\Delta\rho_p/\Delta\rho_m$=10	7.25841	2.69321	1.93613
$\Delta\rho_p/\Delta\rho_m$=20	6.81734	4.90278	2.04411

Notes: Maximum values of the dimensionless number densities of micro-organisms and particles, as well as the maximum value of the dimensionless stream function in the computational domain at steady-state conditions for $D_p/D_m = 0.1$ for different densities of solid particles (based on the data shown in Figures 2, 5, 9, and 10)

Table V.

References

Batchelor, G.K. (1982), "Sedimentation in a dilute polydisperse system of interacting spheres. Part 1. General theory", *Journal of Fluid Mechanics*, Vol. 119, pp. 379-408.

Ghorai, S. and Hill, N.A. (1999), "Development and stability of gyrotactic plumes in bioconvection", *Journal of Fluid Mechanics*, Vol. 400, pp. 1-31.

Ghorai, S. and Hill, N.A. (2000), "Periodic arrays of gyrotactic plumes in bioconvection", *Physics of Fluids*, Vol. 12, pp. 5-22.

Kessler, J.O. (1985a), "Hydrodynamic focusing of motile algal cells", *Nature*, Vol. 313, pp. 218-20.

Kessler, J.O. (1985b), "Co-operative and concentrative phenomena of swimming micro-organisms", *Contemporary Physics*, Vol. 26, pp. 147-66.

Kessler, J.O., Burnett, G.D. and Remick, K.E. (2000), "Mutural dynamics of swimming micro-organisms and their fluid habitat", in Christiansen, P.L., Sorensen, M.P. and Scott, A.C. (Eds), *Nonlinear Science at the Dawn of the 21st Century*, Springer, New York, NY, pp. 409-26.

Kessler, J.O., Wiseley, D.A., Remick, K.E. and Marthaler, D.E. (1997), "Individual and collective dynamics of swimming bacteria", in Schreckenberg, M. and Wolf, D.E. (Eds), *Proceedings of the Workshop "Traffic and Granular Flow'97"*, Springer, New York, NY, pp. 37-51.

Kuznetsov, A.V. and Avramenko, A.A. (2004), "Effect of small particles on the stability of bioconvection in a suspension of gyrotactic microorganisms in a layer of finite depth", *International Communications in Heat and Mass Transfer*, Vol. 31, pp. 1-10.

Pedley, T.J., Hill, N.A. and Kessler, J.O. (1988), "The growth of bioconvection patterns in a uniform suspension of gyrotactic micro-organisms", *Journal of Fluid Mechanics*, Vol. 195, pp. 223-338.

Pedley, T.J. and Kessler, J.O. (1987), "The orientation of spheroidal micro-organisms swimming in a flow field", *Proceedings of the Royal Society of London*, B231, pp. 47-70.

Pedley, T.J. and Kessler, J.O. (1990), "A new continuum model for suspensions of gyrotactic micro-organisms", *Journal of Fluid Mechanics*, Vol. 212, pp. 155-82.

Pedley, T.J. and Kessler, J.O. (1992), "Hydrodynamic phenomena in suspensions of swimming micro-organisms", *Annual Review of Fluid Mechanics*, Vol. 24, pp. 313-58.